

Contents lists available at ScienceDirect

Journal of Experimental Marine Biology and Ecology

journal homepage: www.elsevier.com/locate/jembe



Wasting disease and static environmental variables drive sea star assemblages in the Northern Gulf of Alaska



Brenda Konar^{a,*}, Timothy James Mitchell^a, Katrin Iken^a, Heather Coletti^b, Thomas Dean^c, Daniel Esler^d, Mandy Lindeberg^e, Benjamin Pister^f, Benjamin Weitzman^{a,d}

- ^a University of Alaska Fairbanks, PO Box 757220, Fairbanks, AK 99709, USA
- b US National Park Service, Inventory and Monitoring Program, Southwest Alaska Network, 4175 Geist Road, Fairbanks, AK 99709, USA
- ^c Coastal Resource Associates, 5190 El Arbol Dr., Carlsbad, CA 92008, USA
- ^d US Geological Survey, Alaska Science Center, 4210 University Drive, Anchorage, AK 99508, USA
- e NOAA Fisheries, AFSC, Auke Bay Laboratories, 17109 Pt Lena Loop Rd, Juneau, AK 99801, USA
- f US National Park Service, Kenai Fjords National Park, 411 Washington Street, Seward, AK 99664, USA

ABSTRACT

Sea stars are ecologically important in rocky intertidal habitats where they can play an apex predator role, completely restructuring communities. The recent sea star die-off throughout the eastern Pacific, known as Sea Star Wasting Disease, has prompted a need to understand spatial and temporal patterns of sea star assemblages and the environmental variables that structure these assemblages. We examined spatial and temporal patterns in sea star assemblages (composition and density) across regions in the northern Gulf of Alaska and assessed the role of seven static environmental variables (distance to freshwater inputs, tidewater glacial presence, exposure to wave action, fetch, beach slope, substrate composition, and tidal range) in influencing sea star assemblage structure before and after sea star declines. Environmental variables correlated with sea star distribution can serve as proxies to environmental stressors, such as desiccation, attachment, and wave action. Intertidal sea star surveys were conducted annually from 2005 to 2018 at five sites in each of four regions that were between 100 and 420 km apart across the northern Gulf of Alaska. In the pre-disease years, assemblages were different among regions, correlated mostly to tidewater glacier presence, fetch, and tidal range. The assemblages after wasting disease were different from those before the event with lower diversity and lower density. In addition to these declines, the disease manifested itself at different times across the northern Gulf of Alaska and did not impact all species uniformly across sites. Post sea star wasting, there was a shift in the event with lower diversity and lower density. In addition to these declines, the disease manifested itself at different times across the northern Gulf of Alaska and did not impact all species uniformly across sites. Post sea star wasting, there was a shift in the event with slope, fetch, and tidal range. In essence, sea star wasting disease resulted in a shift in the sea star assemblage that is no

1. Introduction

Intertidal organisms must accommodate extreme conditions, such as high wave action, desiccation, temperature stress (Helmuth and Hofmann, 2001; Sanford, 2002), and intense competition for space (Dayton, 1971). Nevertheless, this habitat supports diverse communities, which include sea stars (Chenelot et al., 2007). Intertidal sea stars can differ in ecological roles, with some species having large-scale impacts on the structure and function of their community (Menge et al., 1994; Moritsch and Raimondi, 2018). The disproportionately large impact that sea stars can have on intertidal community structure has been well documented for *Pisaster ochraceus* in the northeast Pacific, from which the keystone species concept was founded (Paine, 1966). The intense predation by this species on mussels reduces primary substrate availabilty by moderating the density of mussels and opening

space for other species (Paine, 1966; Lafferty and Suchanek, 2016). Because sea stars can play such a pivotal role in structuring intertidal communities, changes to their distribution and abundance can have habitat-wide impacts.

The structure of sea star assemblages can be influenced by environmental variables (Menge and Sutherland, 1987; Petes et al., 2008; Seabra et al., 2011). For example, salinity can correlate strongly with echinoderm distribution in rocky nearshore environments globally (Iken et al., 2010; Agüera et al., 2015); *P. ochraceus* can acclimate to low salinity environments, although this will slow their feeding and mobility rates (Held and Harley, 2009). While some environmental variables are dynamic in nature (e.g., temperature and salinity), many are static and do not vary widely over time. Static variables, including wave exposure and fetch can impose strong physical forces in the intertidal environment, and wave splash can allow invertebrates to exist

E-mail address: bhkonar@alaska.edu (B. Konar).

^{*} Corresponding author.

higher in the intertidal zone by reducing desiccation (Paine, 1974). Some sea stars, such as P. ochraceus can respond with an alteration of their body shape to better withstand high wave action (Hayne and Palmer, 2013). Sea stars with this ability may dominate at high energy beaches. In addition, beach slope and substrate type influence wave action and can affect sea star reproduction and thermoregulation, which in turn can control distribution, abundance and feeding rates, thereby structuring intertidal communities (Ricciardi and Bourget, 1999; Gedan et al., 2011; Bloch and Klingbeil, 2016). Species that occupy a high tidal elevation experience increased intertidal exposure, translating to increased desiccation along with amplified thermal and osmotic stress. Because of the potential importance of static environmental variables in structuring rocky intertidal communities, we examined the effects of seven static variables (distance to freshwater, tidewater glacial presence, wave exposure, fetch, beach slope, substrate composition, and tidal range) on sea star distribution and abundance. A better understanding of these variables will promote development of a framework to explain underlying reasons for large-scale changes and small-scale variability in sea star distribution.

Around 20 sea star species from Mexico to Alaska experienced rapid numerical declines, beginning in Washington and California in the summer of 2013 (Hewson et al., 2014). Termed "Sea Star Wasting Disease" (hereafter "SSWD"), symptomatic sea stars display abnormal twisting of appendages, followed by formation of white lesions and deflation of arms and body, progressing to arm loss, necrosis, disintegration, and death over the course of days to weeks (Eisenlord et al., 2016). Species response to SSWD has been generally negative at both the individual (symptomatic individuals at a given site) and sometimes population level (all individuals of a particular species being impacted in a given region); however, there is much variability in the response of each species across space (Kay et al., 2019; Schultz, 2018; Hewson et al., 2018; Moritsch and Raimondi, 2018; Montecino-Latorre et al., 2016; and also Multi-Agency Rocky Intertidal Network; http://www. seastarwasting.org.accessed 14 Dec. 2018). This recent SSWD epidemic was not novel; however, the geographic range, number of species affected, and rate of mortality were several times greater than described during previous events (Menge et al., 2016). Initial research suggested a viral pathogen, specifically a densovirus called Parvoviridae, which was named the Sea Star Associated Densovirus (SSaDV) (Hewson et al., 2014). More recently, research is pointing to a complex suite of factors including changes to and an imbalance in sea star microbiomes with disease onset (Lloyd and Pespeni, 2018) and environmental stressors (Hewson et al., 2018). One such stressor, temperature, has been correlated with SSWD in some areas and in some sea star species (Harvell et al., 2019). Recent ocean warming trends such as the Pacific marine heatwave, may be an important environmental stressor proliferating the disease (Harvell et al., 2019; Eisenlord et al., 2016; Hewson et al., 2018; Miner et al., 2018). In general though, SSWD does not appear to impact species similarly across their geographic range (Kay et al., 2019; Schultz, 2019). Some sea star species, including Pisaster spp. and Evasterias troschelii may not exhibit SSWD symptoms when they are exclusively exposed to viral pathogens associated with the disease. In contrast, some species such as Pynopodia helianthoides, can exhibit symptoms through only viral pathogen exposure irrespective of environmental conditions (Hewson et al., 2018). Sometimes it takes exposure to pathogens in addition to environmental stressors for symptoms to manifest (Hewson et al., 2018).

The northern Gulf of Alaska (nGOA) is the coldest region and has the most variable temperature in the Pacific Ocean (Stabeno et al., 2004). It is regulated by wind- and freshwater-driven down-welling and counterclockwise flow of the Alaska Coastal Current (Stabeno et al., 2004). The study area, ranging from 58° to 60° N latitude, includes many different coastal habitats. Some regions within the nGOA are influenced by the presence of tidewater glaciers where cold, sediment-laden and stratified waters can be traced at least 10 km from their glacial sources and influence local productivity and ecosystem structure

(Arimitsu et al., 2016). Other regions are protected from wind and waves while still others are exposed. Slope and substrate vary from steep rocky faces to boulder fields and shallow mudflats with cobbles. The tidal range differs among regions within the nGOA, but overall the nGOA has large tidal swings that can work synergistically with wind and current to further increase intertidal disturbance (Ladd et al., 2005). The environmental variability of this study area may enable prediction of the sea star assemblages.

We used sea star assemblage structure data collected prior to, during, and after the onset of SSWD to ask what impact SSWD has had on nGOA sea star assemblages. We also examined if and how static environmental variables correlate with sea star distribution and abundance in the nGOA pre- and post-SSWD. Changes in the static environmental variables most highly correlated with sea star assemblages after the onset of SSWD symptoms may suggest environmental conditions that are favorable for particular sea star species that were less affected by the disease. Finally, we described the current status of sea star assemblages and consider implications of this die off.

2. Methods

2.1. Study area

Four regions throughout the nGOA were surveyed as part of the Gulf Watch Alaska (GWA) research program (https://gulfwatchalaska.org/; Fig. 1). Katmai National Park and Preserve (KATM; 59° N, 155° W) lies on the Alaska Peninsula across Shelikof Strait from the Kodiak Archipelago. It does not have tidewater glaciers but does have indirect glacial input and is indirectly connected to the nGOA. Kachemak Bay (KBAY; 59.5° N and 151° W) is an estuary connected to Cook Inlet, which, compared to other regions, has little exposure to the nGOA but its inner bay is exposed to glacier runoff. Kenai Fjords National Park (KEFJ; 60° N, 150° W) stretches along the southeastern side of the Kenai Peninsula. It is exposed to the open nGOA and has steep slopes leading to deep glacial fjords, some of which have tidewater glaciers. Western Prince William Sound (WPWS; 60° N, 148° W) is a protected and glaciallyinfluenced complex of islands and bays that is connected to (but protected from) the nGOA. These four regions are located between 100 and 420 km apart from each other, with KATM as the farthest west region, followed by KBAY, then KEFJ, with WPWS as the eastern-most region.

Each of the four regions contained five sites. The KATM sites were Amalik Bay, Kaflia Bay, Kinak Bay, Kukak Bay, and Takli Island and were sampled from 2006 to 18, excluding years 2007 and 2011. The KBAY sites were Bluff Point, Cohen Island, Elephant Island, Outside Beach, and Port Graham and were sampled 2005–18, though there were years around 2011 and 2013 where one or more of the KBAY sites were not sampled. The KEFJ sites were Aialik Bay, Harris Bay, McCarty Bay, Nuka Bay, and Nuka Passage and were all sampled 2008–18. The WPWS sites were Herring Bay, Hogan Bay, Iktua Bay, Johnson Bay, and Whale Bay and were all sampled in 2007 and 2010–18.

2.2. Intertidal surveys

Initial sites were selected based on slope, substrate, and extent (at least 100 m of continuous rocky habitat). To varying degrees, all sites were semi-protected and associated with freshwater sources, and a lack of high wave exposure. Monitoring of intertidal sea stars followed a standardized protocol during May to early July low tide series annually (https://www.gulfwatchalaska.org/monitoring/nearshore-ecosystems/). At KATM, KEFJ, and WPWS one $50\,\mathrm{m}\times4\,\mathrm{m}$ swath was sampled horizontally along the beach with the lower boundary of the swath at 0.0 MLLW (Dean and Bodkin, 2011). In KBAY, the mid and low intertidal zones (centered at approximately $+1.5\,\mathrm{and}+0.5\,\mathrm{m}$, respectively, relative to MLLW) were sampled separately along one $50\,\mathrm{m}\times2\,\mathrm{m}$ swath in each stratum and then combined to obtain a sea star density metric comparable to the other regions. Along each swath, all exposed

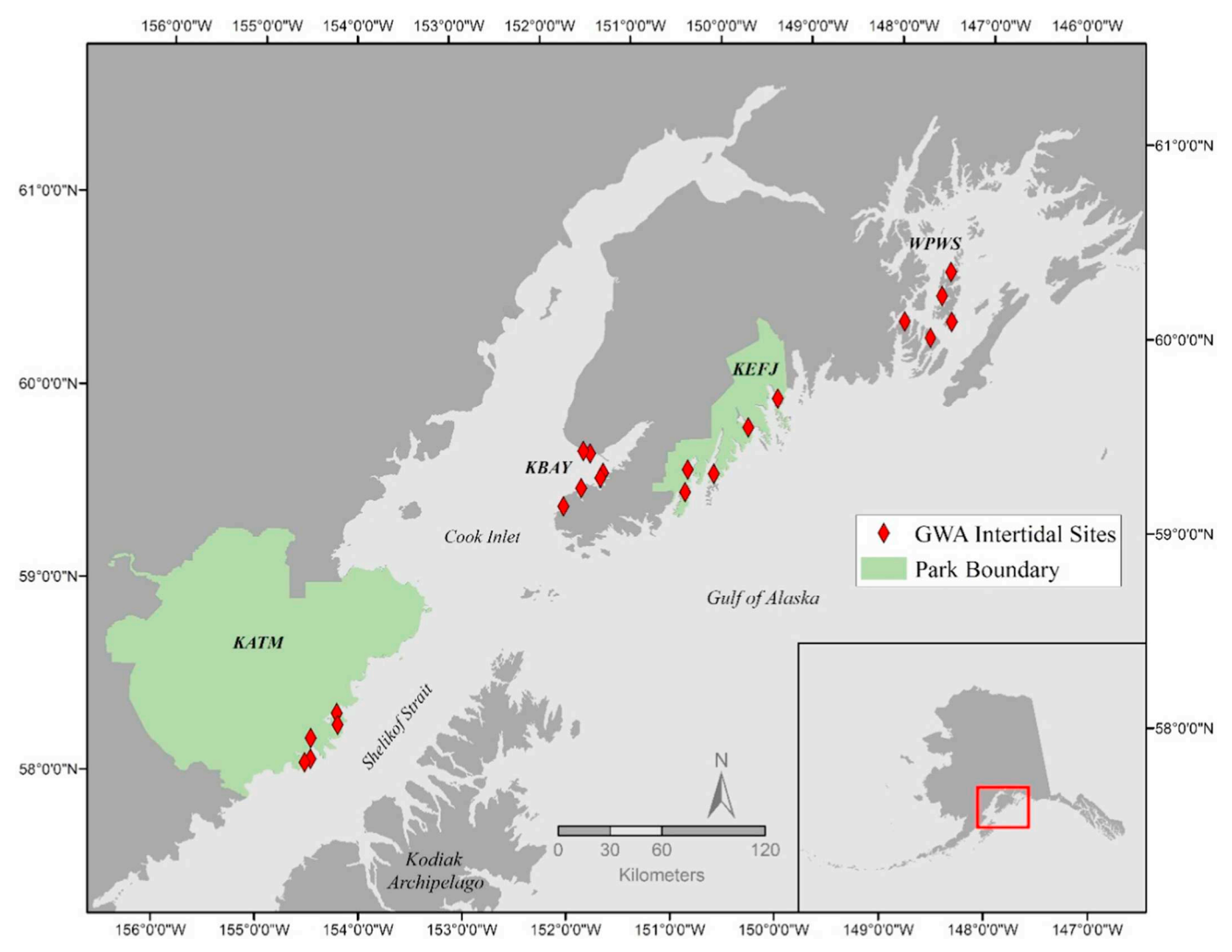


Fig. 1. Map derived from Konar et al. (2016) showing study sites (red diamonds) within the northern Gulf of Alaska: Katmai (KATM), Kachemak Bay (KBAY), Kenai Fjords (KEFJ), and Western Prince William Sound (WPWS). (For interpretation of the references to color in this figure legend, the reader is referred to the web version of this article.)

sea stars were identified and quantified without disturbing the environment. Small cryptic sea stars (e.g., *Leptasterias spp.*) were not quantified. Once symptomatic sea stars were seen in a region, monitoring for sea star disease state was added to field observations.

2.3. Static environmental variables

The static environmental variables used in this analysis included distance to fresh water source, tidewater glacial presence by region, wave exposure, slope, fetch, substrate type, and tidal range and were calculated for a previous study (Konar et al., 2016). In summary, freshwater sources, including the presence of tidewater glaciers, were obtained from the National Hydrography Dataset (NHD; http:// akhydro.uaa.alaska.edu/data/nhd/), a comprehensive set of digital spatial data that includes marine and coastal information created in the early 2000s for Alaska. To standardize distance measurements to fresh water sources, data layers, including shoreline data layers, were rasterized by creating an equal number and size of pixels (50 m \times 50 m pixel size). Using ArcGIS Spatial Analyst Cost Distance tool (ESRI, Redlands, CA), distances from sampling sites to the nearest freshwater source within each region were calculated across water bodies at the exclusion of land masses. This includes only those sources of flowing water that appear on USGS maps and excludes small freshwater discharges on beaches and static bodies of water. Tidewater glacier locations were also obtained from the NHD and were classified as being present or absent in each region. While both the distance to fresh water inputs and the presence of tidewater glaciers are static elements, we recognize that discharge rates can be highly variable. These discharge rates were not included in this study; however, the presence was still deemed important as a source of freshwater. Exposure to wave action was determined from the ShoreZone Alaska data portal (http://www. shorezone.org/), where locations are classified based on the Biological Wave Exposure classifications of protected, semi-protected, or semiexposed (Harper and Morris, 2014). A mean slope (degrees) was calculated for each site in all regions by measuring the distance across every 1 m vertical rise, from below 0.0 MLLW to supratidal zone, at five equidistant points along the 50 m transect and averaging the five calculated slopes. Fetch is another commonly used proxy for the wave exposure of a shore (Burrows et al., 2012; Mieszkowska et al., 2013; Tam and Scrosati, 2014) and provides a continuous scale of potential wave energy. Fetch was calculated by creating vertices every 10° for 360° centered on each study site (i.e., spoke pattern) to a length of 200 km. Vertices were clipped once a land mass was encountered. A sum of the remaining vertices' distances was used to estimate the total potential fetch in km at each site. Two buffers were created around each site to evaluate the effect of small rocks or islets on any particular site:

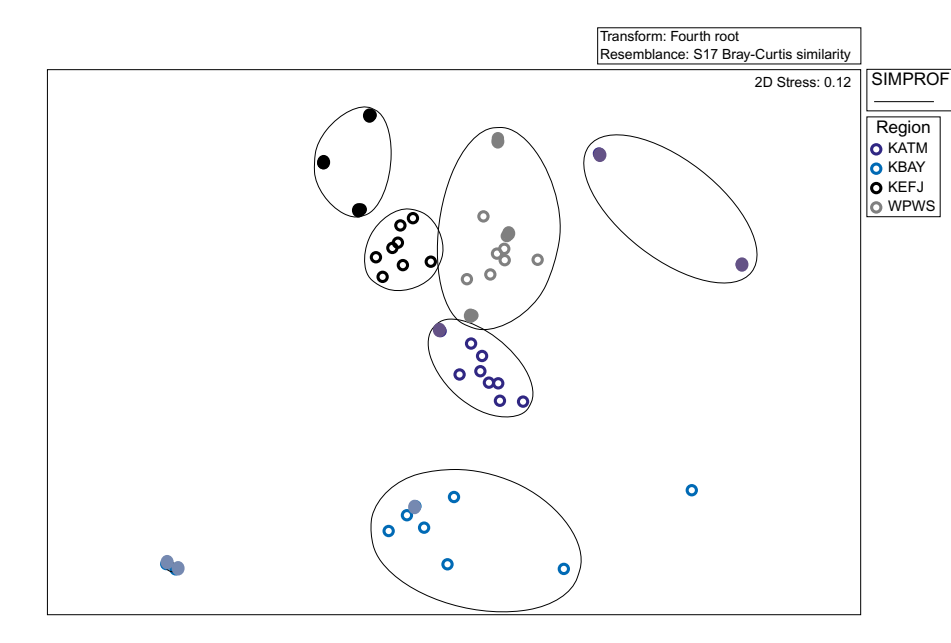


Fig. 2. nMDS ordination plot of sea star assemblages for sites averaged by region and year from 2005 to 18 with SIMPROF groupings (Pi = 5.62, p = .001). 2016–2018 (post-SSWD) are designated by solid symbols and illustrate change in assemblage structure concurrent with disease impact. Regions are color-coded to designate west (blue shades) and east (grey/black shades) zones in the nGOA.

200 m and 5000 m. All land masses that fell within these distances were erased for the respective distance fetch measurements. This allowed calculation of fetch distance after removing potentially ineffective barriers to wave energy. Substrate type was visually estimated as percent substrate cover within 10 randomly placed quadrats in each of the 0.5 and 1.5 strata at each site (n = 20 total) so that a mean could be calculated by site. Substrate categories used the Wentworth scale and included percent of bedrock, boulder, cobble, gravel, mud/sand (Wentworth, 1922). Tidal range was the average distance between MHW and MLW. A larger value designates a greater tidal range, which indicates a larger intertidal zone in areas with similar slopes. These ranges were obtained from the National Oceanic and Atmospheric Administration (NOAA) tides and currents datums (https:// tidesandcurrents.noaa.gov/datums.html?id = 9465953, accessed 20 Nov, 2018). Not all sites are monitored by oceanographic instruments; hence, site tidal range was obtained for all available sites and those numbers were averaged over the respective region (three sites at KATM, one at KBAY, two at KEFJ, and one at WPWS).

2.4. Data analyses

Primer v. 7 was used for all statistical analyses (PRIMER-e, Quest Research Ltd). First, all sea star densities were fourth-root transformed to more equally weight rare species. Resemblance matrices of the sea star assemblages were calculated using Bray-Curtis similarity. The analysis among years necessitated averaging all fourth-root transformed densities over a combined factor of year and region. From this resemblance matrix, data were visualized using a non-metric multidimensional scaling (nMDS) plot with SIMPROF groups, which show structure within the plot based on dendrogram node distances. A year by region crossed ANOSIM was used to test for significant differences between 2012 and 2018 (p < .05). These years were chosen because they had the most similar sampling effort (i.e., all sites were sampled in all years). The species of symptomatic sea stars and their relative declines (averaged across sites within each year) were both found to differ between the two western regions (KATM and KBAY) and the two eastern regions (KEFJ and WPWS) so for some analyses western and eastern regions were separated as zones. The environmental variable data were square-root transformed and normalized. For testing correlation of the biological data with environmental variables as well as similarity among regions, sites were kept separate in the resemblance matrix. From this site-separated resemblance matrix, BioEnv tests were done pre-SSWD (2005-13) and post-SSWD (2017-18 for regions within the western zone and 2016-18 for regions within the eastern zone) to determine which of our targeted environmental static variables correlated with the sea star assemblages (species composition and density). These post-SSWD years were chosen based on the timing of greatest sea star density declines, which occurred in the western zone beginning in 2017 but in the eastern zone beginning in 2015 and 2016. The environmental variables were then added as vectors to a nMDS to visualize correlations of each variable to the observed sea star assemblages. Two ANOSIM tests of sea star assemblages were conducted between zones; one for 2012-13 (pre-SSWD), and one for 2017-18 (post-SSWD). These years were determined by data availability (transect surveys completed in all four regions beginning in 2012) and the same year groups for "pre-SSWD" and "post-SSWD" across the two zones (west and east) were used for the ANOSIM. Therefore, 2012-13 represented a completely sampled and disease-unaffected time for both zones and 2017-18 represented a time at which both zones had experienced declines.

3. Results

3.1. Regional sea star assemblage changes

Each surveyed region in the nGOA had different sea star assemblages (Fig. 2). Although there was much within region variability particularly in the early years, regions underwent noticeable changes in structure beginning in 2016 in the western zone and 2015 in the eastern zone (Figs. 3 and 4). Pre-SSWD (2005–13), sea stars were abundant in all regions with 6–8 different species per region. Post-SSWD, sea star assemblages in all regions were affected, with mostly 2–5 species remaining, although assemblages in each region were affected differently by the disease (Fig. 4).

Symptomatic sea stars were first observed in the nGoA in 2014. They first occurred along the transects in the western zone (KBAY only) in 2016 (although they were observed outside of the transects in 2015), while in the two regions in the eastern zone (KEFJ and WPWS) symptomatic sea stars first occurred in 2014 and 2015, respectively. Both west and east zones experienced sharp declines in overall sea star density the year following the first symptomatic star observation (Fig. 3). In the years pre-SSWD (2012–13) and post-SSWD (2017–18), the east and west zones were significantly different from one another; however, ANOSIM R-values decreased from 0.608 pre-SSWD to 0.246 post-SSWD.

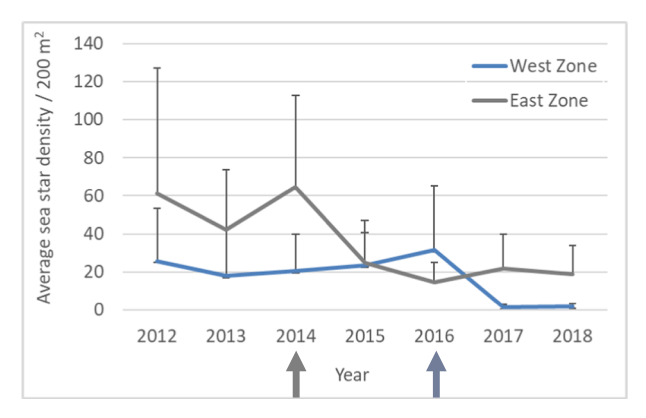


Fig. 3. Yearly densities averaged over the western and eastern zones (+ 1 s.e.). KATM and KBAY indicated by blue line (west). KEFJ and WPWS indicated by grey line (east). Arrows indicate the first sampling year where symptomatic stars were observed (2014 at KEFJ and 2016 at KBAY). (For interpretation of the references to color in this figure legend, the reader is referred to the web version of this article.)

At KATM and KBAY, overall sea star densities declined by 92% and 97%, respectively, from 2016 to 2017. At KEFJ, sea star density dropped by 68% from 2015 to 2016, and at WPWS, sea star density dropped by 64% from 2014 to 2015. Pre-SSWD, KATM had seven total sea star species, with the assemblage being dominated by *E. troschelii* (Fig. 4a). Densities of *E. troschelii* reached as high as 85.0 stars/200 m² at Amalik Bay in 2012. In 2016, the first year that assemblage changes were evident, *E. troschelii* in KATM declined to an average of 3.0 stars/200 m² and *P. ochraceus* and *P. helianthoides* became the most prevalent species. *Pisaster ochraceus* increased from 6.2 stars/200 m² in 2012 to 11.0 in 2016, and *P. helianthoides* slightly increased from 7.6 stars/200 m² in 2012 to 9.6 in 2016 (Figs. 4a and 5). From 2016 to 2017, there was a steep decline in the densities of all KATM sea star species. These data suggest that the overall sea star assemblage changes did not manifest until the summer of 2017, which is corroborated by the

SIMPROF groupings where 2017 and 2018 separated from all previous years (Fig. 2). In KATM, there were nine statistically significant assemblage differences between years – the most of any region (Table 1). Sea star assemblage in years 2017 and 2018 were significantly different from nearly all previous years but not from each other (Table 1). No symptomatic sea stars were observed during any of the annual sampling at KATM, although this was most likely an artifact of sampling.

Prior to SSWD, eight total sea star species were present in KBAY. In 2012, E. troschelii and Henricia leviuscula were the species of highest density (Fig. 5). One individual Lethasterias nanimensis was found at one site (Cohen Island) in 2015 and not seen again at this site or any other region. The first symptomatic stars were seen in 2016, coincident with a large increase of E. troschelii (over 75% of all stars observed), with densities of 28.6 stars/200 m². By the next year, E. troschelii was absent at all five sites within KBAY. Years 2017 and 2018 had overall low densities of all sea stars, with H. leviuscula now being the dominant sea star (Fig. 5). Despite symptomatic sea star presence in 2016 (Fig. 4b), assemblage-wide impacts of the disease seemed to manifest only in 2017 and 2018. The assemblage grouping of KBAY contained a SIM-PROF group with these two years, which were highly similar to each other but different from the previous years (Fig. 2). Sea star assemblages in years 2017 and 2018 were significantly different from most previous years but not from each other (Table 1). Pisaster ochraceus and P. helianthoides were present in very low densities prior to SSWD at KBAY ($< 1 \text{ star}/200 \text{ m}^2$) and absent after the event.

KEFJ had the earliest observed symptomatic stars in the summer 2014 sampling period (Fig. 4c). Pre-SSWD, there were eight total sea star species present with *P. ochraceus*, *P. helianthoides*, and *Dermasterias imbricata* being the dominant species (Fig. 5). One *Mediaster aequalis* individual was found in 2008 at one site (McCarty) and never seen again in this or any other region. All species began to decline in 2015 and continued this trend until 2016 (Fig. 4c). The SIMPROF analysis placed years 2016, 2017, and 2018 in one group and all other years in a separate group (Fig. 2). Assemblages in years 2016 and 2017 were significantly different from those in 2013 and 2014 (Table 1). *Pisaster ochraceus* declined from 30.2 stars/200 m² in 2012 to 6.2 stars/200 m²

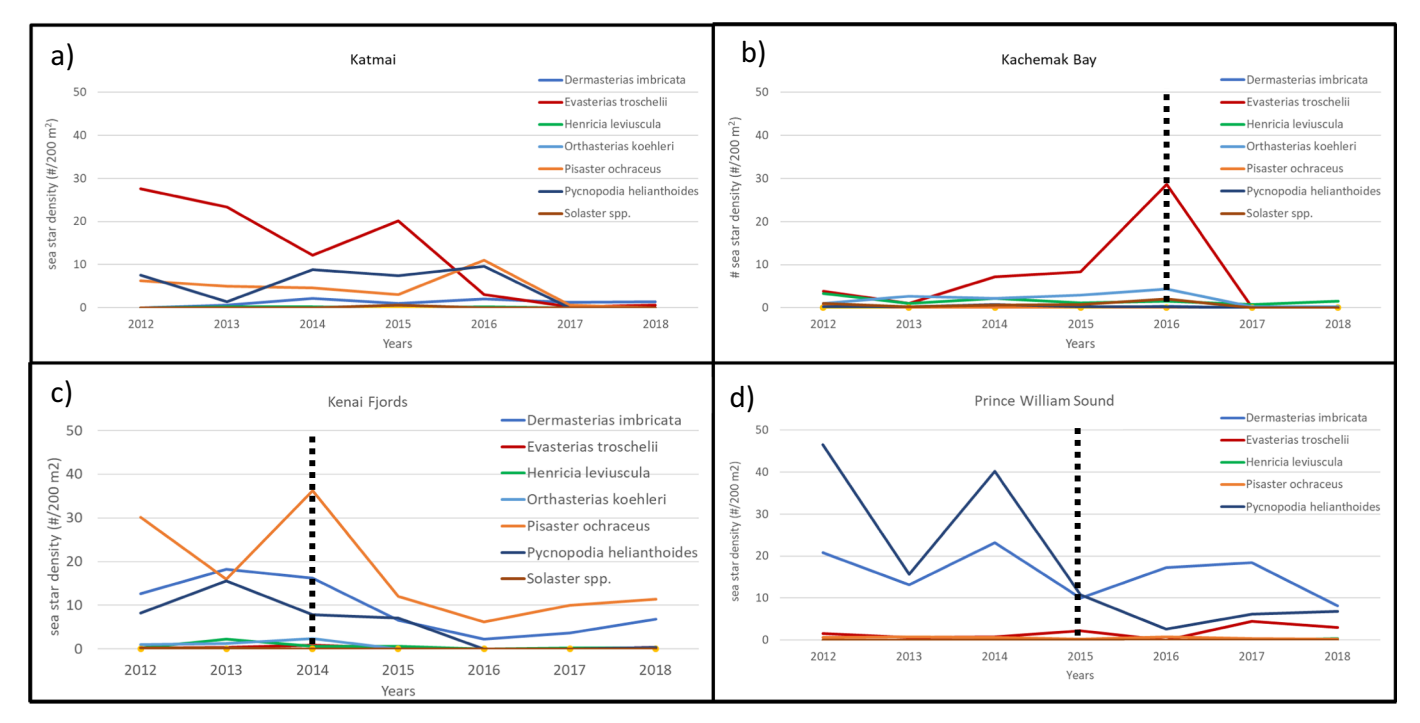


Fig. 4. Changes in sea star density (number of stars/200 m²) by species averaged over sites for each region from 2012 to 18 with the western zone on top – KATM (a) and KBAY (b), and the eastern zone on bottom – KEFJ (c) and WPWS (d). The first year that a sea star exhibiting symptoms of wasting disease was observed in the transects is denoted by a dashed line in each region.

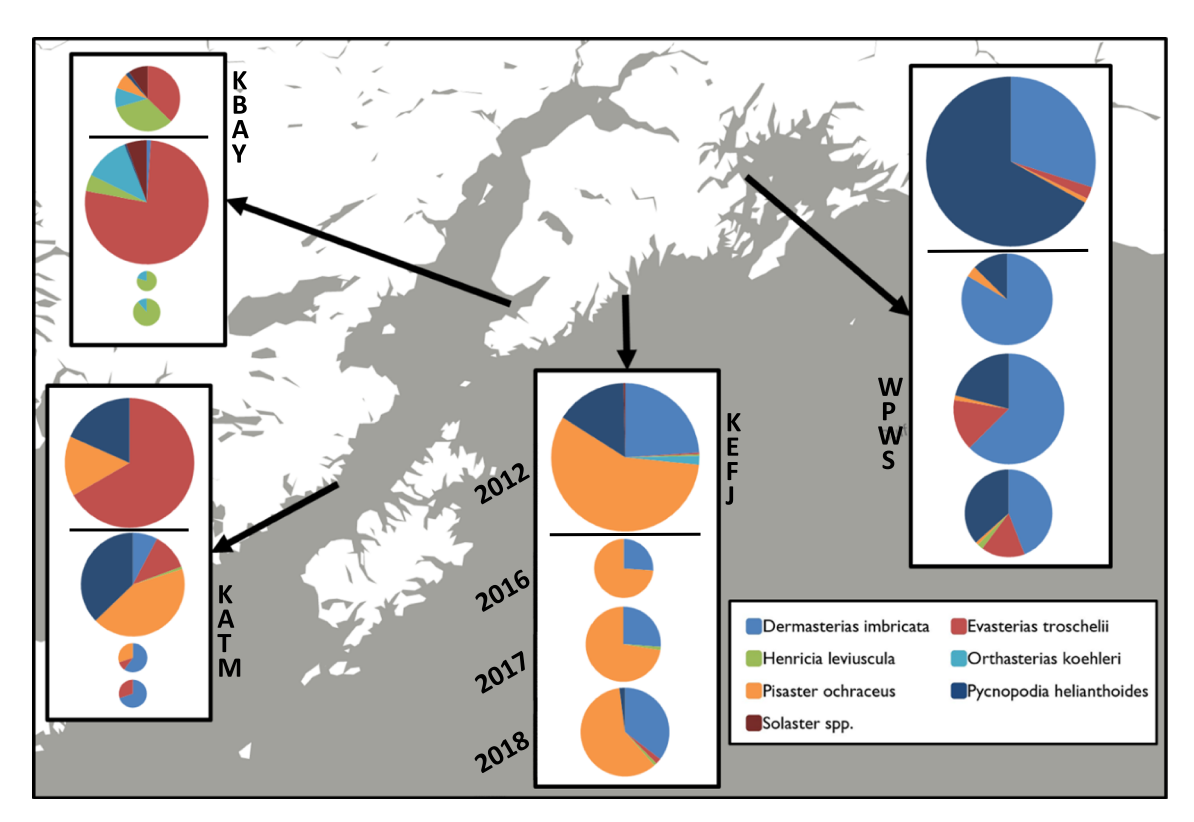


Fig. 5. Sea star distribution across regions, going from left to right: KATM, KBAY, KEFJ, and WPWS. The four pie charts from each region going from top to bottom are 2012, 2016, 2017, 2018. The black line indicates a break in consecutive years. The sizes of the pies are scaled to total sea star abundance to show abundance trends among years as well as among regions. This illustrates the changes that took place in the sea star assemblage pre- (2012) and post- (all other years) onset of SSWD. No regions exhibited evidence of SSWD in 2012. By 2016, KEFJ and WPWS exhibited sea star declines and symptomatic sea stars were seen at KBAY that year. Years 2017 and 2018 display assemblages that have been impacted by SSWD among all four regions.

Table 1 ANOSIM R-values (first number) and p-values (second number) comparing differences in sea star assemblages between years at each region. Significant values (p < .05) in bold.

	2012	2013	2014	2015	2016	2017
2013	-0.040, 0.548					
	-0.064, 0.698				■KATM	
	-0.025, 0.484				■KBAY	
	-0.132, 0.849		-		■KEFJ	
2014	0.068, 0.222	-0.048, 0.667			1 —	
	-0.268, 0.960	-0.036, 0.603			■WPWS	
	0.060, 0.270	0.000, 0.381				
	-0.188, 1.000	-0.088, 0.651		1		
2015	-0.056, 0.683	-0.036, 0.579	-0.172, 0.929			
	-0.272, 0.984	0.016, 0.389	-0.024, 0.476			
	-0.084, 0.635	-0.072, 0.603	-0.064, 0.627			
	-0.084, 0.698	0.072, 0.278	0.032, 0.437		1	
2016	0.096, 0.206	0.124, 0.167	-0.188, 0.921	-0.132, 0.865		
	0.600, 0.016	0.236, 0.111	0.608, 0.024	0.564, 0.024		
	-0.116, 0.730	-0.013, 0.437	0.196, 0.119	-0.028, 0.508		
	0.184, 0.135	0.432, 0.004	0.400, 0.008	0.316, 0.071		
2017	0.928, 0.008	0.648, 0.008	0.294, 0.071	0.674, 0.016	0.414, 0.040	
	0.100, 0.238	-0.048, 0.651	0.136, 0.183	0.092, 0.238	-0.032, 0.468	
	0.520, 0.016	0.259, 0.127	0.522, 0.048	0.51, 0.024	0.440, 0.032	
	0.140, 0.159	0.364, 0.040	0.352, 0.008	0.304, 0.063	-0.142, 0.825	
2018	0.744, 0.008	0.772, 0.016	0.408, 0.048	0.668, 0.016	0.460, 0.048	0.008, 0.365
	0.052, 0.325	0.152, 0.111	0.094, 0.151	-0.032, 0.659	0.420, 0.024	-0.028, 0.508
	0.520, 0.016	0.244, 0.143	0.458, 0.056	0.502, 0.024	0.440, 0.040	-0.128, 1.000
	-0.046, 0.619	0.140, 0.143	0.016, 0.389	0.052, 0.317	-0.100, 0.786	-0.168, 0.873

in 2016 but subsequently increased in 2018 to 11.4 stars/200 m² – about 38% of pre-SSWD densities. *Dermasterias imbricata* went from an average of 18.2 stars/200 m² in 2013 down to 2.2 stars/200 m² in 2016 and back up to 6.8 stars/200 m² in 2018. As of 2018, *P. helianthoides* was still absent from KEFJ except for one site, Aialik Bay, where there were 2.0 stars/200 m². Through the whole SSWD event, *P. ochraceus* maintained its position as the dominant species at KEFJ, with *D. imbricata* making up 25% to 30% of the assemblage each year (Fig. 5).

In WPWS, pre-SSWD, there were five total sea star species (Fig. 4d). Symptomatic sea stars were first seen in 2015 (Fig. 4d). This is the only region where *P. helianthoides* was the dominant species pre-SSWD and the only region that never showed a complete absence of *P. helianthoides* during annual surveys (Fig. 4d). While decreasing from an average of 46.6 stars/200 m² in 2012 to just 2.6 stars/200 m² in 2016, *P. helianthoides* has since begun to increase, with 6.8 stars/200 m² in the 2018 survey (Fig. 4d). In 2016, *D. imbricata* increased and became the dominant species (Fig. 5). The SIMPROF grouping placed every year of this region in the same group with assemblages in 2016 and 2018 being the most separated (Fig. 2). Sea star densities in 2016 were significantly different from densities in 2012, 2014, and 2015 and 2018 (Table 1).

3.2. Static environmental variable correlations

Before SSWD symptoms appeared (2005-2013), tidewater glacier presence, fetch (using the 200 m buffer), and tidal range had the strongest BioEnv correlation with sea star assemblages (Spearman Rank Coefficient [rho] of 0.730) (Fig. 6). The two sites within the western zone were free of tidewater glaciers while some sites within the eastern zone had nearby tidewater glaciers. After SSWD (2017-18 for KATM and KBAY; 2016-18 for KEFJ and WPWS), correlation coefficient with environmental variables was similar (rho = 0.703) and included slope, fetch (using the 200 m buffer), and tidal range with the strongest correlations. Of the five remaining species post-SSWD, three inhabited sites with similar fetch, slope, and tidal range, Evasterias troschelii, D. imbricata, and P. helianthoides were all remaining at sites with average fetch between 67 km and 88 km, slope between 31.9 and 34.2°, and tidal range of 2.81 to 2.88 m. In contrast, H. leviuscula was remaining at sites with average fetch of 762 km, slope of 15°, and tidal range of 3.85 m. Pisaster ochraceus was present at sites with average fetch at 200 m of 178 km, slope of 23.8°, and tidal range of 2.66 m.

4. Discussion

Across a wide range of latitudes (approximately 80° S to 70° N), there are typically no more than five total intertidal echinoderm species present in a region (Iken et al., 2010), with more tropical areas in the western Pacific having 0–5 species (Lambert, 2000; Pearse, 2009). However, pre-SSWD, sea star species richness was higher at nGOA study sites, which included 6–8 species per region. These sea star assemblages were slightly less rich than more southern assemblages in Puget Sound, WA, with a richness of ten species. Pre-SSWD species composition was also fundamentally different across the study regions in the nGOA. The dominant sea stars in the nGOA pre-SSWD included *D. imbricata, E. troschelii, P. ochraceus*, and *P. helianthoides*. These species all have wide geographic ranges spanning the northeastern Pacific (Lambert, 2000).

SSWD did not impact regions in the nGOA simultaneously, but sequentially, with declines seen in the regions in the eastern zone first followed by the regions in the western zone. Although species richness in each region decreased due to SSWD, assemblage structure became slightly more similar across regions, likely due to overall fewer species in all regions. The cause of SSWD can be different across species and geographic ranges (Hewson et al., 2018); however, ocean temperature may be a contributor to SSWD outbreaks (Eisenlord et al., 2016; Kohl et al., 2016). It has been hypothesized that ocean warming trends, particularly the anomalously high ocean temperatures on the US west coast in 2013–15, acted as a regime shift, causing a stress-induced

decline in sea star abundances in some areas for some sea star species (Burt et al., 2018). The nGOA experienced colder than normal temperatures in 2013, when the western US coast was seeing warm ocean temperatures and the beginning of the massive sea star disease outbreak. The next year (2014), a three-year anomalous warm spell manifested at the intertidal sites in the nGOA (Coletti et al., 2018; Monson, 2018) concomitant with the first observations of symptomatic sea stars. While the reasons for the time lag between the east and west zones are unknown, this does align with the progression of this SSWD epidemic. The disease was first recorded in P. ochraceus on the coast of Washington in June 2013 but later that year was observed affecting several sea star species along the Washington and California coasts (Hewson et al., 2014). It then progressed to Oregon, where it was first encountered in April 2014 (Menge et al., 2016). It was first seen in the nGOA transects in 2014 in KEFJ and progressed westward to KBAY transects in 2016 (although it was observed in the KBAY area in 2015). Although experimental laboratory results have been inconclusive (Hewson et al., 2018), increased temperature has been shown to affect the progression and speed of SSWD for some species in certain regions (Eisenlord et al., 2016; Kohl et al., 2016).

As the nGOA appears to be experiencing cooler ocean temperatures in recent years as compared to the warm temperatures experienced at the beginning of the sea star disease outbreak (Coletti et al., 2018), sea star assemblages may be able to rebound. If this recent cooling continues into the future, then sea stars may be less stressed, which may assist in their recovery. While stress could be from warm temperatures alone, it is more likely a suite of environmental parameters leading to the stress and ultimate infection of these species. For *P. helianthoides*, exposure to wasting asteroid-associated densoviruses with no change in environmental conditions and no added stress is enough to elicit SSWD so it is unclear if and how cooler temperatures will enhance the recovery of this species (Hewson et al., 2018). It is also unclear how this recent cooling will affect other sea star populations along their geographic range since so little SSWD-related immune response research has been conducted on species other than *P. helianthoides*.

Static environmental variables of rocky intertidal habitats can drive community structure. In the GoA, we found that pre-SSWD, sea star assemblages were highly correlated with the presence of tidewater glaciers, fetch (200 m buffer distance), and tidal range. Tidewater glacier presence may lead to low salinity, low temperature, and high sedimentation (Urbanski et al., 2017). In the nGOA, D. imbricata, P. helianthoides, and P. ochraceus were more abundant in regions that had tidewater glaciers. Studies on the effects of low salinity on P. ochraceus suggest that this species may be able to acclimate to low salinity as acclimated sea stars have been found to feed, move, and survive better in a hyposaline environment than non-acclimated animals of the same species (Held and Harley, 2009). Sedimentation can disrupt feeding and respiration in some invertebrates, although glacial-associated sea star species appear to tolerate it (Newcombe and Macdonald, 1991). Fetch (a metric of wave exposure) also correlated with sea star assemblages in the nGOA. High fetch results in a more extreme intertidal environment with frequent disturbance from wind and wave action (Seapy and Littler, 1978). Pre-SSWD, sea stars such as D. imbricata, P. helianthoides, and P. ochraceus were associated with more protected environments (lower fetch). For P. helianthoides, sea star size can be positively correlated with wave exposure (fetch), with juveniles residing in protected waters and adults in semi-exposed and exposed areas (Shivji et al., 1983). Size was not measured in this study, so similar trends with size and exposure could not be explored. Lastly, tidal range was found to correlate with sea star assemblages in this study. The KBAY tidal range was very large relative to the other regions and was positively correlated with E. troschelii abundance, although this was largely driven by a single year that had very high abundances of this species. The exposure tolerance of sea stars is largely unknown but may explain why the KBAY sea star assemblage often appears to be different from the other regions. Some species, such as P. helianthoides and D. imbricata, were uncommon

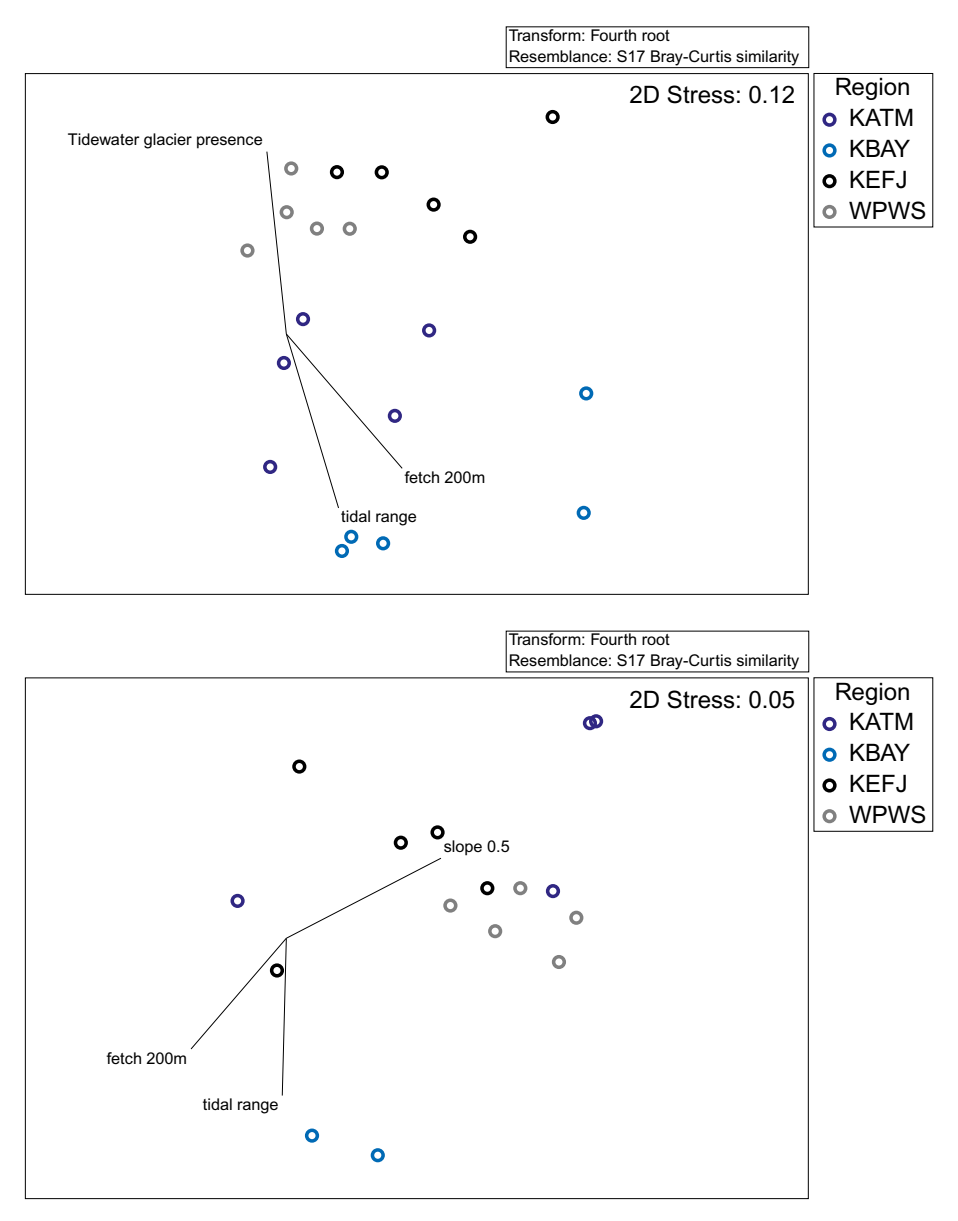


Fig. 6. nMDS ordination plots of sites with years averaged over pre-SSWD (top) (2005–13 for all regions) and post-SSWD (bottom) (2017–18 for KATM and KBAY; 2016–18 for KEFJ and WPWS) sea star assemblages with vectors indicating the highest correlated environmental variables as related to sites. Regions are color-coded to designate west (blue shades) and east (grey/black shades) zones in the nGOA. Takli Island, Bluff Point, Cohen Island, and Elephant Island were excluded from the post-SSWD analyses because no sea stars were found at these sites and here we illustrate which environmental variables correlated with the remaining sea stars.

in the intertidal around KBAY but were common at intertidal sites with lesser tidal range and also were common in the subtidal around KBAY pre-SSWD (Iken et al., 2010; pers. comm, Konar).

The sea star assemblages post-SSWD were correlated with similar environmental variables as pre-SSWD, except tidewater glacier presence was replaced by slope. This new correlated environmental variable may be related to the remaining sea star species being less influenced by tidewater glaciers and more correlated to slope. Two of the three species that correlated with tidewater glaciers pre-SSWD, *P. helianthoides* and *P. ochraceus*, were largely eliminated in the nGOA by SSWD. The absence of these species most likely explains the change in this correlated environmental variable. In general *D. imbricata, E. troschelii*, and *P. helianthoides* were more correlated with sites that had steep slopes while *P. ochraceus* correlated with moderate slopes and *H. leviuscula* correlated with shallow slopes. How slope directly impacts these species is unknown but it could be acting as a proxy for wave action and/or exposure to air.

Similar to many regions in the north Pacific, SSWD had a profound

impact on all nGOA study regions. In the past, SSWD outbreaks have manifested themselves several times (Bates et al., 2009; Eckert et al., 2000), with this current epidemic having the greatest spatial impact on the highest number of species (Hewson et al., 2014). For example, Heliaster kubiniji was decimated by SSWD in the Gulf of California several decades ago during a period when abnormally warm, fresh water was present (Dungan et al., 1982). In the face of future SSWD epidemics, some populations in more suitable habitats (so they are less stressed) may experience fewer casualties, while populations in suboptimal habitats (and are already stressed) will see greater declines. While this may favor certain species overall, it will be highly dependent on location and the extent and type of environmental stress encountered. This study provides a basis for understanding the static environmental variables acting on intertidal sea star assemblages across the nGOA and will allow for greater power to interpret how dynamic environmental variables that may be stressors, such as water temperature, influence sea star assemblage structure.

In Alaska, the keystone role of sea stars can resemble that of sea

otters, which are often the most important predator in coastal communities (Estes and Duggins, 1995). As such, sea stars can exert topdown control on food webs (Vicknair and Estes, 2012). Co-predator dynamics that arise from multiple predators competing for similar resources have elucidated the ecologically important role of P. helianthoides, even in the presence of a keystone predator like the sea otter. For example, in rocky reef habitats of British Columbia, SSWD mortality of P. helianthoides released medium and small sized sea urchins from top-down control and allowed for an outbreak of sea urchin barrens, even in the presence of sea otters (Burt et al., 2018). Another example from heterogeneous habitats in Kachemak Bay showed sea stars, in addition to sea otters, were important consumers of clams (Traiger et al., 2016). The decline of sea stars in the nGOA could influence the abundance of potential prey items such as clams or sea urchins, with ecosystem level implications (Burt et al., 2018). Declines in certain species of sea star will have different levels of impact on surrounding species interactions. For example, P. helianthoides is a highly mobile predator, with the ability to chemosense prey, and regulate the abundance of lower trophic animals (Brewer and Konar, 2005). The sea stars found in the nGOA likely play important roles in structuring nearshore benthic communities and their decline may have direct impacts on their prey and the surrounding community.

Since the nGOA intertidal zones were devoid of sea stars for multiple years, increases in secondary consumers and prey may be occurring as has been seen in other areas affected by SSWD (Burt et al., 2018; Gravem and Morgan, 2017; Schultz et al., 2016). Depending on the recovery rate of sea star populations, particularly predatory stars such as P. ochraceus and P. helianthoides, the intertidal may lose overall diversity as competitively dominant prey species increase in the absence of predation. Systems that lose a top predator but retain a less efficient competitor species can exhibit prey increases through apparent predator release (Cerny-Chipman et al., 2017). SSWD-induced declines of P. helianthoides in British Columbia, Canada were followed by trophic cascades characterized by 300-400% increases in sea urchins and significant decreases in kelp cover (Burt et al., 2018; Schultz et al., 2016). In Oregon, P. ochraceus density was reduced by as much as 84%, which led to a decline in mussel predation rate (Menge et al., 2016). This decline was immediately followed by an unprecedented, large recruitment event of P. ochraceus, which may have allowed restoration of predation pressure prior to a regime shift or trophic cascade (Menge et al., 2016). However, smaller stars exert much lower predation pressure, especially on large prey, than adults (Menge et al., 2016). In the nGOA in 2018, 110 small sea stars (arm radius < 5 mm of E. troschelii, P. helianthoides, D. imbricata) were counted across three of the study regions (KATM, KEFJ, and WPWS; https://gulfwatchalaska.org/ monitoring/) and in 2019, small E. troschelii and P. helianthoides were seen in the subtidal areas in KBAY (Konar pers. obs.), indicating potential initial recovery. While outside the scope of this study, a future study examining intertidal community diversity pre- and post-SSWD in the nGOA regions might provide insight into the overall community changes. A study of this type would also help elucidate the importance of the various sea star species to intertidal community structure as they may begin to recover in the various sites and regions.

Acknowledgements

We thank all the student and other volunteers who assisted with the field work associated with this project. We also thank the scientific team of the Gulf Watch Alaska long-term monitoring program for their expertise and resources in support of this publication. The research described in this manuscript was supported by the *Exxon Valdez* Oil Spill Trustee Council. However, the findings and conclusions presented by the authors are their own and do not necessarily reflect the views or position of the Trustee Council. Any use of trade, firm, or product names is for descriptive purposes only and does not imply endorsement by the U. S. Government.

References

- Agüera, A., Schellekens, T., Jansen, J.M., Smaal, A.C., 2015. Effects of osmotic stress on predation behaviour of Asterias rubens L. J. Sea Res. 99, 9–16. https://doi.org/10. 1016/j.seares.2015.01.003.
- Arimitsu, M.L., Piatt, J.F., Mueter, F., 2016. Influence of glacier runoff on ecosystem structure in Gulf of Alaska fjords. Mar. Ecol. Prog. Ser. 560, 19–40. https://doi.org/ 10.3354/meps11888.
- Bates, A.E., Hilton, B.J., Harley, C.D.G., 2009. Effects of temperature, season and locality on wasting disease in the keystone predatory sea star *Pisaster ochraceus*. Dis. Aquat. Org. 86, 245–251. https://doi.org/10.3354/dao02125.
- Bloch, C.P., Klingbeil, B.T., 2016. Anthropogenic factors and habitat complexity influence biodiversity but wave exposure drives species turnover of a subtropical rocky intertidal metacommunity. Mar. Ecol. 37, 64–76. https://doi.org/10.1111/maec.12250.
- Brewer, R., Konar, B., 2005. Chemosensory responses and foraging behavior of the seastar Pycnopodia helianthoides. Mar. Biol. 147, 789–795. https://doi.org/10.1007/s00227-005-1608-7.
- Burrows, M.T., Jenkins, S.R., Robb, L., Harvey, R., 2012. Spatial variation in size and density of adult and post-settlement *Semibalanus balanoides*: effects of oceanographic and local conditions. Mar. Ecol. Prog. Ser. 398, 207–219.
- Burt, J.M., Tinker, M.T., Okamoto, D.K., Demes, K.W., Holmes, K., Salomon, A.K., 2018. Sudden collapse of a mesopredator reveals its complementary role in mediating rocky reef regime shifts. Proc. R. Soc. B Biol. Sci. 285, 1–9. https://doi.org/10.1098/rspb. 2018.0553.
- Cerny-Chipman, E., Sullivan, J., Menge, B., 2017. Whelk predators exhibit limited population responses and community effects following disease-driven declines of the keystone predator *Pisaster ochraceus*. Mar. Ecol. Prog. Ser. 570, 15–28. https://doi.org/10.3354/meps12121.
- Chenelot, H., Iken, K., Konar, B., Edwards, M., 2007. Spatial and temporal distribution of echinoderms in rocky nearshore areas of Alaska. Publ. Seto. Mar. Biol. Lab. Spec. Publ. Ser. 8, 11–28. https://doi.org/10.5134/70914.
- Coletti, H., Bodkin, J., Dean, T., Iken, K., Konar, B., Monson, D., Esler, D., Lindeberg, M., Suryan, R., 2018. Intertidal ecosystem indicators in the northern Gulf of Alaska. In: Zador, S., Yasumiishi, E. (Eds.), Ecosystem Considerations 2018: Status of the Gulf of Alaska Marine Ecosystem. Report, North Pacific Fishery Management Council, 605 W 4th Ave, Suite 306, Anchorage, AK 99301.
- Dayton, P.K., 1971. Competition, disturbance, and community organization: the provision and subsequent utilization of space in a rocky intertidal community. Ecol. Monogr. 41, 351–389.
- Dean, T.A., Bodkin, J.L., 2011. SOP for sampling of intertidal invertebrates and algae on sheltered rocky shores - Version 4.6: Southwest Alaska Inventory and Monitoring Network. Natural Resource Report NPS/SWAN/NRR—2011/397. National Park Service. Fort Collins. Colorado.
- Dungan, M.L., Miller, T.E., Thomson, D.A., 1982. Catastrophic decline of a top carnivore in the Gulf of California rocky intertidal zone. Science 216, 989–991.
- Eckert, G.L., Engle, J.M., Kushner, D.J., 2000. Sea star disease and population declines at the Channel Islands. In: Proceedings of the Fifth California Islands Symposium, pp. 390–393.
- Eisenlord, M.E., Groner, M.L., Yoshioka, R.M., Elliott, J., Maynard, J., Fradkin, S., Turner, M., Pyne, K., Rivlin, N., van Hooidonk, R., Harvell, C.D., 2016. Ochre star mortality during the 2014 wasting disease epizootic: role of population size structure and temperature. Philos. Trans. R. Soc. Lond. Ser. B Biol. Sci. 371, 20150212. https://doi.org/10.1098/rstb.2015.0212
- Estes, J.A., Duggins, D.O., 1995. Sea otters and kelp forests in Alaska: generality and variation in a community ecological paradigm. Ecol. Monogr. 65, 75–100. https:// doi.org/10.2307/2937159.
- Gedan, K.B., Bernhardt, J., Bertness, M.D., Leslie, H.M., 2011. Substrate size mediates thermal stress in the rocky intertidal. Ecology 92, 576–582. https://doi.org/10.1890/ 10-0717.1.
- Gravem, S.A., Morgan, S.G., 2017. Shifts in intertidal zonation and refuge use by prey after mass mortalities of two predators. Ecology 98, 1006–1015. https://doi.org/10. 1002/ecv.1672.
- Harper, J., Morris, M., 2014. Alaska ShoreZone coastal habitat mapping protocol. In: Contract Report prepared by Coastal & Oceans Resources Inc., Archipelago Marine Research Ltd. and Nuka Research and Planning, LLC. Bureau of Ocean Energy, Anchorage, AK for the. (164 p).
- Harvell, C.D., Montecino-Latorre, D., Caldwell, J.M., Burt, J.M., Bosley, K., Keller, A., Heron, S.F., Salomon, A.K., Lee, L., Pontier, O., Pattengill-Semmens, C., 2019. Disease epidemic and a marine heat wave are associated with the continental-scale collapse of a pivotal predator (*Pycnopodia helianthoides*). Science Advances 5 (1) (p.eaau7042).
- Hayne, K.J.R., Palmer, A.R., 2013. Intertidal sea stars (*Pisaster ochraceus*) alter body shape in response to wave action. J. Exp. Biol. 216, 1717–1725. https://doi.org/10.1242/ jeb.078964.
- Held, M.B.E., Harley, C.D.G., 2009. Responses to low salinity by the sea star *Pisaster ochraceus* from high- and low-salinity populations. Invertebr. Biol. 128, 381–390. https://doi.org/10.1111/j.1744-7410.2009.00175.x.
- Helmuth, B.S.T., Hofmann, G.E., 2001. Microhabitats, thermal heterogeneity, and patterns of physiological stress in the rocky intertidal zone. Biol. Bull. 201, 374–384.
- Hewson, I., Button, J.B., Gudenkauf, B.M., Miner, B., Newton, A.L., Gaydos, J.K., Wynne, J., Groves, C.L., Hendler, G., Murray, M., Fradkin, S., Breitbart, M., Fahsbender, E., Lafferty, K.D., Kilpatrick, A.M., Miner, C.M., Raimondi, P., Lahner, L., Friedman, C.S., Daniels, S., Haulena, M., Marliave, J., Burge, C.A., Eisenlord, M.E., Harvell, C.D., 2014. Densovirus associated with sea-star wasting disease and mass mortality. Proc. Natl. Acad. Sci. U. S. A. 111, 17278–17283. https://doi.org/10.1073/pnas.

1416625111.

- Hewson, I., Bistolas, K.S.I., Quijano Cardé, E.M., Button, J.B., Foster, P.J., Flanzenbaum, J.M., Kocian, J., Lewis, C.K., 2018. Investigating the complex association between viral ecology, environment, and northeast Pacific sea star wasting. Front. Mar. Sci. 5, 1–14. https://doi.org/10.3389/fmars.2018.00077.
- Iken, K., Konar, B., Benedetti-Cecchi, L., Cruz-Motta, J.J., Knowlton, A., Pohle, G., Mead, A., Miloslavich, P., Wong, M., Trott, T., Mieszkowska, N., Riosmena-Rodriguez, R., Airoldi, L., Kimani, E., Shirayama, Y., Fraschetti, S., Ortiz-Touzet, M., Silva, A., 2010. Large-scale spatial distribution patterns of echinoderms in nearshore rocky habitats. PLoS One 5, 1–14. https://doi.org/10.1371/journal.pone.0013845.
- Kay, S.W.C., Gehman, A.-L.M., Harley, C.D.G., 2019. Reciprocal abundance shifts of the intertidal sea stars, Evasterias troschelii and Pisaster ochraceus, following sea star wasting disease. Proc. R. Soc. B286, 20182766.
- Kohl, W.T., McClure, T.I., Miner, B.G., 2016. Decreased temperature facilitates short-term sea star wasting disease survival in the keystone intertidal sea star *Pisaster ochraceus*. PLoS One 11, e0153670. https://doi.org/10.1371/journal.pone.0153670.
- Konar, B., Iken, K., Coletti, H., Monson, D., Weitzman, B., 2016. Influence of static habitat attributes on local and regional rocky intertidal community structure. Estuar. Coast. 39, 1735–1745. https://doi.org/10.1007/s12237-016-0114-0.
- Ladd, C., Stabeno, P., Cokelet, E.D., 2005. A note on cross-shelf exchange in the northern Gulf of Alaska. Deep. Sea. Res. Part. II Top. Stud. Oceanogr. 52, 667–679.
- Lafferty, K.D., Suchanek, T.H., 2016. Revisiting Paine's 1966 sea star removal experiment, the most-cited empirical article in the American Naturalist. Am. Nat. 188, 365–378.
- Lambert, P., 2000. Sea Stars of British Columbia, Southeast Alaska, and Puget Sound. UBC Press, Vancouver.
- Lloyd, M.M., Pespeni, M.H., 2018. Microbiome shifts with onset and progression of Sea Star Wasting Disease revealed through time course sampling. Sci. Rep. 8, 16476.
- Menge, B.A., Sutherland, J.P., 1987. Community regulation: variation in disturbance, competition, and predation in relation to environmental stress and recruitment. Am. Nat. 130, 730–757.
- Menge, B.A., Berlow, E.L., Blanchette, C.A., Navarrete, S.A., Yamada, S.B., 1994. The keystone species concept: variation in interaction strength in a rocky intertidal. Ecol. Monogr. 64, 249–286.
- Menge, B.A., Cerny-Chipman, E.B., Johnson, A., Sullivan, J., Gravem, S., Chan, F., 2016. Sea star wasting disease in the keystone predator *Pisaster ochraceus* in Oregon: insights into differential population impacts, recovery, predation rate, and temperature effects from long-term research. PLoS One 11, e0153994. https://doi.org/10.6085/AA/.
- Mieszkowska, N., Milligan, G., Burrows, M.T., Freckleton, R., Spencer, M., 2013. Dynamic species distribution models from categorical survey data. J. Anim. Ecol. 82, 1215–1226.
- Miner, C.M., Burnaford, J.L., Ambrose, R.F., Antrim, L., Bohlmann, H., Blanchette, C.A., Engle, J.M., Fradkin, S.C., Gaddam, R., Harley, C.D.G., Miner, B.G., Murray, S.N., Smith, J.R., Whitaker, S.G., Raimondi, P.T., 2018. Large-scale impacts of sea star wasting disease (SSWD) on intertidal sea stars and implications for recovery. PLoS One 13, e0192870. https://doi.org/10.1371/journal.pone.0192870.
- Monson, D.H., 2018. Gulf of Alaska intertidal temperature anomalies. In: Zador, S., Yasumiishi, E. (Eds.), Ecosystem Status Report 2018: Gulf of Alaska, Stock Assessment, and Fishery Evaluation Report, North Pacific Fishery Management Council. 605 West 4th Ave. Suite 306. Anchorage.
- Montecino-Latorre, D., Eisenlord, M.E., Turner, M., Yoshioka, R., Harvell, C.D., Pattengill-Semmens, C.V., Nichols, J.D., Gaydos, J.K., 2016. Devastating transboundary impacts

- of sea star wasting disease on subtidal asteroids. PLoS One 11 (10), e0163190.

 Moritsch, M.M., Raimondi, P.T., 2018, Reduction and recovery of keystone predation
- Moritsch, M.M., Raimondi, P.T., 2018. Reduction and recovery of keystone predation pressure after disease-related mass mortality. Ecol. Evol. 8, 3952–3964.
- Newcombe, C.P., Macdonald, D.D., 1991. Effects of suspended sediments on aquatic ecosystems. North. Am. J. Fish. Manag. 11, 72–82. https://doi.org/10.1577/1548-8675(1991)011 < 0072: EOSSOA > 2.3.CO; 2.
- Paine, R.T., 1966. Food web complexity and species diversity. Am. Nat. 100, 65–75. https://doi.org/10.1086/282400.
- Paine, R.T., 1974. Intertidal community structure. Oecologia 15, 93–120. https://doi.org/ 10.1007/BF00345739.
- Pearse, J.S., 2009. Shallow-water asteroids, echinoids, and holothuroids at 6 sites across the tropical west Pacific, 1988-1989. Galaxea. J. Coral Reef Stud. 11, 1–9. https://doi.org/10.3755/galaxea.11.187.
- Petes, L.E., Mouchka, M.E., Milston-Clements, R.H., Momoda, T.S., Menge, B.A., 2008. Effects of environmental stress on intertidal mussels and their sea star predators. Oecologia 156, 671–680. https://doi.org/10.1007/s00442-008-1018-x.
- Ricciardi, A., Bourget, E., 1999. Global patterns of macroinvertebrate biomass in marine intertidal communities. Mar. Ecol. Prog. Ser. 185, 21–35.
- Sanford, E., 2002. Water temperature, predation, and the neglected role of physiological rate effects in rocky intertidal communities. Integr. Comp. Biol. 42, 881–891. https://doi.org/10.1093/icb/42.4.881.
- Schultz, J.A., 2018. Sea star wasting disease update!. In: Bodtker, K. (Ed.), Ocean Watch B.C. Coast Edition, pp. 1–323.
- Schultz, J.A., Cloutier, R.N., Côté, I.M., 2016. Evidence for a trophic cascade on rocky reefs following sea star mass mortality in British Columbia. Peer J. 4, e1980. https://doi.org/10.7717/peerj.1980.
- Seabra, R., Wethey, D.S., Santos, A.M., Lima, F.P., 2011. Side matters: microhabitat influence on intertidal heat stress over a large geographical scale. J. Exp. Mar. Bio. Ecol. 400, 200–208. https://doi.org/10.1016/j.jembe.2011.02.010.
- Seapy, R.R., Littler, M.M., 1978. The distribution, abundance, community structure, and primary productivity of macroorganisms from two central California rocky intertidal habitats. Pacific Sci. 32, 293–314.
- Shivji, M., Parker, D., Hartwick, B., Smith, M., Sloan, N., 1983. Feeding and distribution study of the sunflower sea star *Pycnopodia helianthoides*. Pacific Sci. 37, 133–140.
- Stabeno, P.J., Bond, N.A., Hermann, A.J., Kachel, N.B., Mordy, C.W., Overland, J.E., 2004. Meteorology and oceanography of the northern Gulf of Alaska. Cont. Shelf Res. 24, 859–897. https://doi.org/10.1016/j.csr.2004.02.007.
- Tam, J.C., Scrosati, R.A., 2014. Distribution of cryptic mussel species (*Mytilus edulis* and *M. trossulus*) along wave exposure gradients on northwest Atlantic rocky shores. Mar. Biol. Res. 10. 51–60.
- Traiger, S., Konar, B., Doroff, A., McCaslin, L., 2016. Sea otters versus sea stars as major clam predators: evidence from foraging pits and shell litter. Mar. Ecol. Prog. Ser. 560, 73–86. https://doi.org/10.3354/meps11871.
- Urbanski, J.A., Stempniewicz, L., Węsławski, J.M., Dragańska-Deja, K., Wochna, A., Goc, M., Iliszko, L., 2017. Subglacial discharges create fluctuating foraging hotspots for sea birds in tidewater glacier bays. Sci. Rep. 7, 1–12. https://doi.org/10.1038/srep43999.
- Vicknair, K., Estes, J.A., 2012. Interactions among sea otters, sea stars, and suspension-feeding invertebrates in the western Aleutian archipelago. Mar. Biol. 159, 2641–2649. https://doi.org/10.1007/s00227-012-2021-7.
- Wentworth, C.K., 1922. A scale of grade and class terms for clastic sediments. J. Geol. 30, 377–392.